



Magnetic activity linked generation of nighttime equatorial spread F irregularities

B. Kakad,^{1,2} K. Jeeva,¹ K. U. Nair,¹ and A. Bhattacharyya¹

Received 14 August 2006; revised 28 March 2007; accepted 17 April 2007; published 27 July 2007.

[1] Results derived from a statistical study of the generation of equatorial spread F (ESF) irregularities as a result of magnetic activity based on spaced receiver ionospheric scintillation data recorded at a dip equatorial station is reported here. For a study of this nature it is essential to establish whether the observed scintillations are caused by freshly generated irregularities or by irregularities generated earlier, which later drift onto the signal path. It has been observed in the past that the maximum cross-correlation between the spaced receiver signals is significantly less than 1 during the initial phase of development of ESF irregularities due to the presence of perturbation electric fields associated with the Rayleigh-Taylor (R-T) instability that produces equatorial plasma bubbles (EPBs), whereas in the later phase, when these perturbation electric fields die down, the correlation between the two signals increases rapidly. This feature is used in the present study to identify freshly generated ESF irregularities associated with EPBs using spaced receiver scintillation data. Magnetically disturbed days are chosen by using three hourly geomagnetic activity index ap , daily index Ap , and also AE index to study the cases of prompt penetration of high-latitude electric field to the equatorial ionosphere. Disturbed time statistical occurrence pattern of freshly generated irregularities shows seasonal variation for all three types of magnetic disturbances: disturbance dynamo, prompt penetration, combination of disturbance dynamo and prompt penetration. However, it is found that fresh generation of the irregularities due to magnetic activity is most likely to occur around midnight hours in all seasons. Suppression of generation of irregularities immediately after sunset due to inhibition of the growth of the R-T instability on the bottomside of the equatorial F region is clearly seen in vernal equinox (March and April) and solstice months but is not observed for autumnal equinox (September and October).

Citation: Kakad, B., K. Jeeva, K. U. Nair, and A. Bhattacharyya (2007), Magnetic activity linked generation of nighttime equatorial spread F irregularities, *J. Geophys. Res.*, 112, A07311, doi:10.1029/2006JA012021.

1. Introduction

[2] The ambient electric field plays a very important role in the dynamics of the equatorial F region. It is well known that the eastward electric field is often enhanced in the postsunset hours before it turns westward. This raises the F layer through an $\mathbf{E} \times \mathbf{B}$ drift to higher altitudes, where ion-neutral collisions are less. Sharp upward density gradient on the bottomside of the F layer due to high recombination rate in the E region and increase in the height of F layer in postsunset hours are favorable for the growth of Rayleigh-Taylor (R-T) plasma instability, resulting in the generation of electron density irregularities. Though the basic conditions required for growth of R-T instability are present every day in the postsunset hours, the generation of equatorial plasma bubbles (EPBs) and

associated irregularities in the equatorial F region described by the term equatorial spread F (ESF) does not occur every day. Nevertheless, height of the postsunset equatorial F region peak has emerged as a key parameter for the occurrence of such irregularities [Jayachandran *et al.*, 1993; Fejer *et al.*, 1999].

[3] During and shortly after periods of enhanced geomagnetic activity, ionospheric electric fields in the equatorial and low latitude ionosphere may be altered significantly. As a result, generation of ESF irregularities in the postsunset hours may get influenced very significantly during magnetically disturbed days. The ionospheric electric field modulated by magnetic activity may assist or suppress the generation of EPBs and associated irregularities in the postsunset hours depending on the direction and strength of disturbed time ionospheric electric fields. During quiet days, free from the effect of magnetic activity, generation of EPBs has been found to be restricted to hours before 2200 LT, whereas cases of freshly generated irregularities observed after 2200 LT were found to be associated with magnetic activity [Bhattacharyya *et al.*, 2002]. The

¹Indian Institute of Geomagnetism, Navi Mumbai, New Panvel, India.

²Formerly B. Engavale.

fresh generation of irregularities after 2200 LT may be associated with a significant increase in the height of the equatorial F layer caused by eastward turning of equatorial F region ionospheric electric field due to (a) the occurrence of both disturbance dynamo and prompt penetration, or (b) a superimposed disturbance dynamo electric field [Blanc and Richmond, 1980], or (c) prompt penetration of an eastward electric field from high to low latitudes during magnetically active period. The altered neutral wind pattern due to enhanced Joule energy in the high-latitude ionosphere during magnetically active periods takes some time to set up a disturbance dynamo affecting the equatorial and low latitude ionosphere, but once set up, the disturbance dynamo electric field generally persists for a longer time duration [Fejer et al., 1990; Fejer and Scherliess, 1995; Fuller-Rowell et al., 2002] than the promptly penetrated electric field. A prompt penetration of high-latitude or magnetospheric electric field into the equatorial ionosphere may reverse the direction of the ambient electric field from westward to eastward during periods of rapid decrease of polar cap potential [Spiro et al., 1988; Fejer et al., 1990]. The purpose of the present work is to study the statistical occurrence pattern of freshly generated EPBs triggered by magnetic activity with different starting time and history and to investigate their local time and seasonal dependence.

[4] The first step in such a study using ionospheric scintillation data is to establish whether observed scintillations are caused due to irregularities that have been generated earlier and later drifted across the signal path or due to freshly generated irregularities. In past studies of the effect of magnetic activity on the generation of ESF irregularities using scintillation data, this point has not been taken into account. This issue is crucial for establishing a cause-effect relationship between magnetic activity and EPBs. Bhattacharyya et al. [2001] were the first to observe that in the early phase of development of an EPB due to growth of the R-T instability development on the bottomside of the equatorial F region, decorrelation between signals from two spaced receivers is very high due to the presence of randomly varying perturbation electric fields associated with the plasma instability itself, later (after around 2200 LT) due to a rapid decrease in the perturbation electric field associated with the plasma instability as the height of the F region decreases, signals from the receivers are found to be highly correlated and the estimated maximum cross correlation of the spaced receiver signals approaches 1. The disturbed time scenario may be different from the quiet time pattern of maximum cross correlation of spaced receiver signals. It has been observed that the estimated maximum cross-correlation may fall well below 1 even after 2200 LT only on magnetically disturbed days, and this feature may be used to identify irregularities that have been freshly generated as a result of magnetic activity [Bhattacharyya et al., 2002]. A large data base of ionospheric scintillations observed on a 251 MHz signal transmitted from a geostationary satellite and recorded at an equatorial station by two spaced receivers closely aligned along the magnetic east-west direction is used here in the first statistical study of the occurrence pattern of freshly generated EPBs as a result of magnetic activity, using the above technique to identify the nascent EPBs.

[5] The effect of magnetic disturbances on equatorial F region plasma drifts is seen as well, over and above the day-to-day variability in the quiet time eastward drift of the ground scintillation pattern, for which a monthly pattern of local time variation is estimated using the spaced receiver data [Bhattacharyya et al., 2002; Engavale et al., 2005]. In the absence of magnetic disturbances, when perturbation electric fields associated with the R-T instability dies down after 2200 LT, irregularities tend to drift with the background plasma as shown in a computer simulation of the evolution of the R-T instability in the presence of a realistic background plasma motion [Retterer, 1999]. The spaced receiver scintillation technique only yields the drift of the ground scintillation pattern, which is determined by the drift of the irregularities across the signal path. However, a comparison of neutral wind and spaced receiver drifts have shown a good correspondence between the two after about 2200 LT [Basu et al., 1996]. Also F region dynamo calculations of the zonal plasma drifts have reproduced fairly well, the average irregularity drifts obtained with the scintillation technique during magnetically quiet conditions [Valladares et al., 1996]. Hence after 2200 LT the estimated drifts of the ground scintillation pattern may be considered to be representative of the ambient plasma drifts if there is no fresh generation of irregularities after 2200 LT. Disturbed time plasma drifts often show very clear departure from monthly average quiet time drift pattern, as indicated by the estimated drift of ground scintillation pattern after 2200 LT. On some occasions the effect of a disturbance dynamo can also be seen on the day following a magnetically disturbed day [Fejer et al., 1991; Bhattacharyya et al., 2002]. Therefore days following days with high magnetic activity, which show the effect of magnetic disturbance on plasma drift are also included as magnetically disturbed days in the present study. Generally, periods with $Kp \geq 3+$ or $ap \geq 18$ are considered as magnetically disturbed periods [Bartels, 1957; Menvielle and Berthelier, 1991].

[6] The technique used for analysis of spaced receiver scintillation data and identification of nascent EPBs is discussed in section 2. The different criteria used to define magnetically disturbed days in the present study are described in section 3. Some specific examples of freshly generated EPBs are presented in section 4 and the statistical results for the occurrence pattern of freshly generated EPBs obtained from scintillation data are discussed in section 5. This is followed in section 6 by a summary of the findings of the present study.

2. Data Analysis and Identification of Freshly Generated Irregularities

[7] Amplitude scintillation data for a 251 MHz signal transmitted from the geostationary satellite, UFO2, located at 71.2°E and recorded by two spaced receivers at the equatorial station, Tirunelveli (dip latitude 0.6°N) for the period June 2001 to January 2006 is used in the present study. In addition to this, amplitude scintillation data on a 251 MHz signal transmitted from the geostationary satellite, FLEETSAT located at 73°E and recorded at Tirunelveli, for the equinoctial and summer months of 1995–2000 have also been included in the study. The sampling rate for both

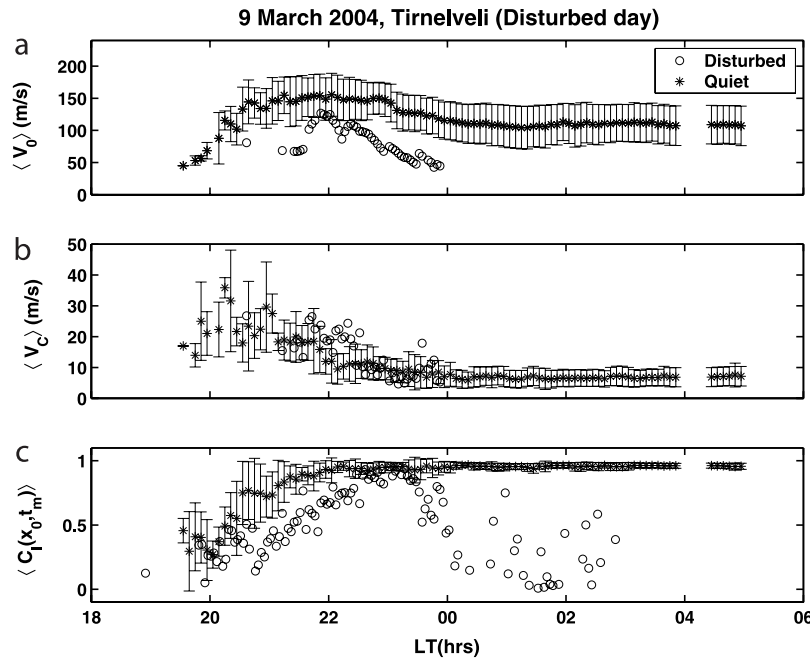


Figure 1. Monthly magnetically quiet time average of drift speed of ground scintillation pattern V_0 , random velocity V_C , and $C_I(x_0, t_m)$ with standard deviation for March 2004, superposed with disturbed time patterns on 9 March 2004 ($\Sigma Kp = 27$, $Ap = 28$).

these sets is 10 Hz. The EPBs and associated irregularities that give rise to the observed scintillations are known to be nearly field-aligned and hence variations in the ground scintillation pattern is expected only in the magnetic east-west direction. The spaced receivers are separated by a distance of 540 m in magnetic east-west direction. Scintillation data from the two receivers are subjected to full correlation analysis, which was introduced by *Brigg* [1984]. In this technique it is assumed that the space-time correlation function of intensity variations has the form:

$$C_I(x, t) = f \left[(x - V_0 t)^2 + V_C^2 t^2 \right] \quad (1)$$

where f is a monotonically decreasing function of its argument with $f(0) = 1$. V_0 is the average drift speed of the scintillation pattern along the receivers' baseline, and random velocity V_C is a measure of random changes in the ground scintillation pattern as it drifts, due to random changes in the irregularity characteristics. The maximum cross-correlation of intensity fluctuations, $C_I(x_0, t_m)$, recorded by the two receivers with a separation of x_0 ; the average drift V_0 ; the random velocity V_C ; and S_4 index, which is the standard deviation of normalized intensity variations, are estimated from the scintillation data for every 3 min interval, for the duration of the scintillation event. In order to eliminate noisy signals from the scintillation data, only 3 min intervals with $S_4 \geq 0.15$ are considered for application of full correlation analysis. When $C_I(x_0, t_m) \geq 0.5$, the assumption regarding the functional form of $C_I(x, t)$ given in equation (1) is expected to be valid around the maximum value of $C_I(x_0, t)$ and hence V_0 and V_C are estimated for only those 3 min intervals, which have $C_I(x_0, t_m) \geq 0.5$. Scintillations observed at a given time may be produced by irregularities that are either generated

freshly or were generated a few hours earlier and later drifted across the signal path. Hence identification of freshly generated irregularities is taken up first in the present study.

[8] As stated earlier, for quiet periods, which do not show any effect of magnetic disturbance, the spaced receiver signals become well correlated after 2200 LT due to the decay of the perturbation electric fields associated with the R-T instability, yielding values of $C_I(x_0, t_m)$ close to 1 [*Bhattacharyya et al.*, 2001]. An example of this is shown in Figure 1, where the monthly pattern of quiet time variation with local time (LT) of V_0 , V_C , and $C_I(x_0, t_m)$ is shown for March 2004 as 6 min averages for all the quiet days with scintillations, together with the standard deviation. Superimposed on this are the values of V_0 , V_C , and $C_I(x_0, t_m)$ for a magnetically disturbed day: 9 March 2004. After 2200 LT, when perturbation electric field associated with the R-T instability vanishes, estimated V_0 may be close to the background zonal plasma drift, as discussed earlier. Disturbance dynamo electric field and prompt penetration of magnetospheric electric field to low latitudes may modulate the height of the equatorial F region significantly during magnetically disturbed conditions. Ionospheric responses are very different during different magnetically active periods [*Dymond et al.*, 2004; *Su. Basu et al.*, 2005; *Basu et al.*, 2005]. This disturbed behavior of the ionosphere on occasion results in the generation of fresh EPBs after 2200 LT when the normally westward electric field changes to eastward, and on some other occasions, the usual post-sunset growth of R-T instability may be suppressed due to westward turning of the normally eastward electric field at this time. Also the disturbance may alter the zonal drift of the background plasma, which shows up as a change in V_0 , the average drift speed of the ground scintillation pattern. On 9 March 2004 the large decrease in $C_I(x_0, t_m)$ starting

around midnight, as seen in Figure 1, indicates fresh generation of an EPB with its associated perturbation electric field. It may be noted that before the EPB was generated the zonal drift clearly showed the effect of a disturbance dynamo. Once the EPB is generated and $C_f(x_0, t_m)$ falls below 0.5, V_0 calculation may not yield accurate results due to deviation from the assumed form of $C_f(x, t)$ given in (1), as mentioned earlier. Hence V_0 values on this day are not available beyond midnight. This is an example of where the effect of disturbance dynamo could be clearly identified before it produce a fresh EPB, which is also clearly identifiable using the decorrelation of spaced receiver scintillation signals.

3. Criteria for Selection of Magnetically Disturbed Days

[9] For the present statistical study, disturbed days are separated from quiet days using three hourly geomagnetic activity index ap and the daily index Ap , which is the average of eight values of ap for each day. These indices are available at <http://swdcd.b.kugi.kyoto-u.ac.jp>. Generally, periods with $Kp \geq 3+$ or $ap \geq 18$ are considered as magnetically disturbed. Nature, evolution, and strength of geomagnetic disturbances are determined by the interplanetary solar wind conditions and interaction of coronal mass ejections (CMEs) and solar wind with Earth's magnetic field [Akasofu, 1981; Lopez et al., 2004]. For the present study, magnetically disturbed days are identified by characteristics that fall in any of the following five categories depending on the nature and starting time of geomagnetic disturbances based on ap and Ap and sometimes AE indices and the local time of the station under consideration:

[10] 1. Category A is days with $Ap \geq 20$ and with at least six intervals that have magnetic disturbances with $ap \geq 18$.

[11] 2. Category B is days for which magnetic activity, as defined by values of $ap \geq 18$, starts at a time later than 1500 LT, irrespective of the duration of magnetic activity. For such days Ap may or may not be less than 20. However, since the magnetic activity starts at a time later than 1000 UT, there would be fewer than six intervals with $ap \geq 18$. Hence such days are not included in category A even if $Ap \geq 20$.

[12] 3. Category C is days on which significant magnetic activity is present only during the period 0500–1500 LT at the longitude sector under consideration ($77.8^\circ E$), which translates to around 0000–1000 UT. For these days Ap may or may not be less than 20, but even if $Ap \geq 20$, they are excluded from category A because of the limited period of magnetic activity.

[13] 4. Category D is days following magnetically disturbed days ($Ap \geq 20$), which are quiet ($Ap < 20$) and also do not fall into category B and C but show the effect of previous day's magnetic disturbances either on zonal plasma drifts or maximum cross-correlation of spaced receiver signals.

[14] 5. Category E is days when it is observed that when conditions are magnetically quiet (i.e., $ap < 18$ approximately for past 36 hours), any sudden and sharp increase in AE of more than 450 nT over a time period of less than 1 hour, resulting in values of AE greater than 500 nT, during 1800–0600 LT, may sometimes give rise to fresh generation of irregularities. This may be an effect of prompt penetra-

tion of a magnetospheric electric field into equatorial ionosphere. Such cases are identified as isolated prompt penetration cases provided the previous days were magnetically quiet and did not fall into categories A, B, or C. In this paper the local time pattern of generation of fresh irregularities due to such promptly penetrated electric fields is studied.

[15] In past studies, often only category A magnetic activity has been considered. Here category B has also been introduced as a criterion for identifying magnetically disturbed days, since this type of magnetic activity is important for the generation of EPBs. It should be noted that the day preceding a magnetically disturbed day of the categories A, B, or C may be magnetically quiet or disturbed. Identification and separation of prompt penetration electric field effects is difficult when prompt penetration takes place during the time when a disturbance dynamo has already been set up by earlier magnetic activity. A recent theoretical study by Maruyama et al. [2005] shows that prompt penetration electric field may alter the midlatitude and low-latitude conductivity and neutral wind, preferentially at night, and this in turn influences subsequent development of a disturbance dynamo. For days included in categories C and D, fresh generation of EPBs after 2200 LT may only take place as a result of a disturbance dynamo producing a net eastward electric field in the equatorial F region at that time. For the E category days, on the other hand, nascent EPBs may only be associated with prompt penetration of an eastward electric field from magnetosphere into the equatorial ionosphere as a result of over shielding at a time of rapid decrease of the polar cap potential. It is for days in A and B categories that it is not possible to attribute the fresh generation of an EPB due to either prompt penetration effect or disturbance dynamo effects. It should be pointed out that even if the preceding day for B and C categories are magnetically disturbed, the effect of the preceding days magnetic activity may only be seen as a disturbance dynamo effect. Hence the above statement regarding fresh generation of EPBs after 2200 LT for categories A and B taken together on one hand and categories C and D taken together on the other hand, are still applicable even if the preceding day for B and C categories are magnetically disturbed.

4. Generation of ESF Irregularities Due to Magnetic Activity

[16] Some examples of fresh generation of irregularities on magnetically disturbed days identified under different categories are discussed in this section. The distribution of (1) maximum cross-correlation, $C_f(x_0, t_m)$, of intensity variations recorded by the spaced receivers for a magnetically disturbed day, 1 October 2002 ($\Sigma Kp = 40$, $Ap = 67$), superimposed on the monthly quiet time average pattern of $C_f(x_0, t_m)$ along with the standard deviation for October 2002, (2) S_4 index on this disturbed day, and (3) ap as a function of UT (UT = LT-5.5 hours) for this disturbed day, which falls under category A, are displayed in Figures 2a, 2b, and 2c. On this magnetically disturbed day, low values of $C_f(x_0, t_m)$ are observed even after 2200 LT, which is considered as an indication of freshly generated irregularities. A similar plot for 3 January 2003 ($\Sigma Kp = 23$, $Ap = 18$)

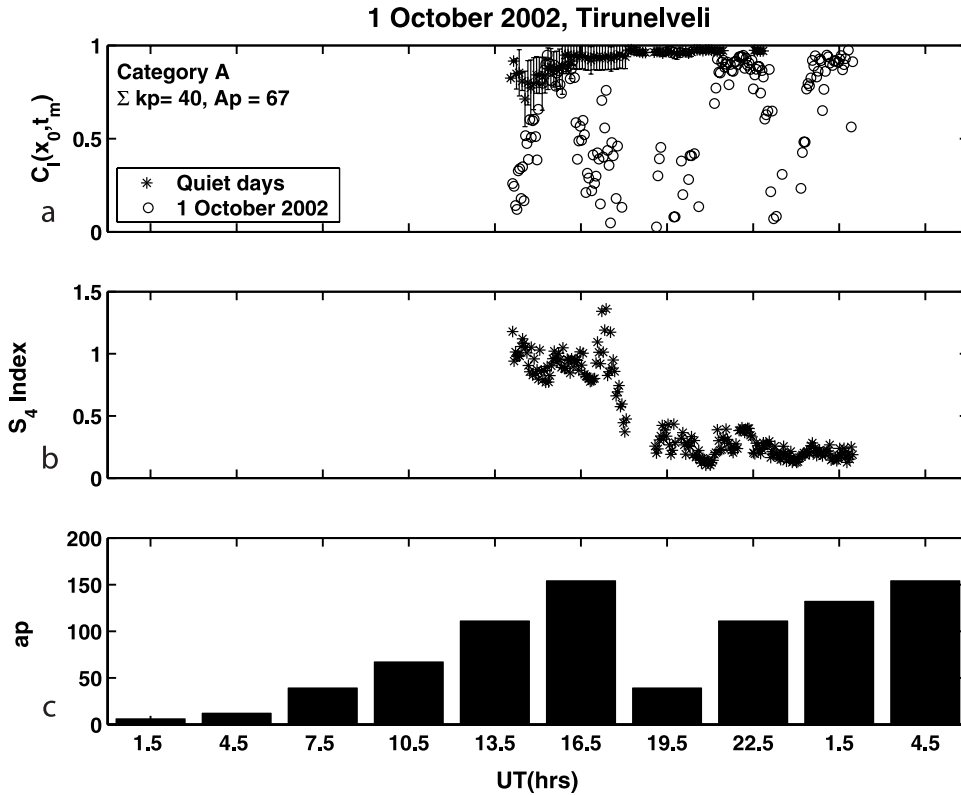


Figure 2. Plot of (a) monthly quiet time average of $C_I(x_0, t_m)$ for October 2002 with standard deviation, superposed with disturbed time $C_I(x_0, t_m)$, (b) S_4 index, and (c) ap indices on 1 October 2002 (Category A) as a function of UT.

is shown in Figure 3. As magnetic activity starts late in the evening around 2200 LT on 3 January 2003, this day is considered under category B. As depicted in the monthly quiet time pattern of $C_I(x_0, t_m)$, scintillations generally start around 1900 LT on quiet days, but on 3 January 2003, scintillations started around 2200 LT, i.e., just after the onset of magnetic activity. The observed scintillations are associated with low values of $C_I(x_0, t_m)$ indicating presence of freshly generated irregularities.

[17] Sometimes effect of magnetic activity may be observed on the day following a magnetically disturbed day. Figure 4 displays variation of (1) $C_I(x_0, t_m)$ along with monthly quiet time average; (2) eastward drift V_0 of ground scintillation pattern along with the monthly quiet time average of V_0 ; and (3) ap as a function of UT for 21 September 2003 ($\Sigma Kp = 26, Ap = 18$), which is a quiet day following a magnetically disturbed day 20 September 2003 ($\Sigma Kp = 31, Ap = 27$). The eastward drift of the ground scintillation pattern shows a clear departure from monthly quiet time pattern after about 2200 LT; even though ap values on this day do not indicate any significant magnetic activity. This implies that the observed decrease in eastward drift of ground scintillation pattern and hence of the irregularities moving along with the background plasma is caused by a disturbance dynamo set up by the previous day's magnetic activity. This disturbance dynamo modifies the zonal electric field as well, which at a later time leads to fresh generation of an EPB on this night. No scintillations

were observed during the period 17–20 September 2003, which was highly disturbed with Ap values of 70, 50, and 39 on 17, 18, and 19 September 2003, respectively. Hence it is possible that generation of ESF irregularities on these days was suppressed by the earlier magnetic activity.

5. Statistics of Freshly Generated ESF Irregularities

[18] Given the basic differences between different magnetically active periods and their wide ranging effects on the nighttime equatorial ionosphere, a statistical study has been undertaken here to obtain a broad picture of the connection between magnetic activity and the generation of EPBs, after application of the new technique to identify nascent EPBs [Bhattacharyya *et al.*, 2002], which forms the crux of such a study. Magnetically active days chosen using the criteria described in section 3 are compiled in different sets depending on the source of the eastward electric field responsible for the fresh generation of EPBs: (1) a possible combination of prompt penetration and disturbance dynamo effects (case a), (2) eastward electric field arising from a disturbance dynamo (case b), and (3) promptly penetrating eastward electric fields (case c). In terms of the five categories of magnetic activity discussed in section 3 that have been used to identify a magnetically disturbed day in the present study, in case c the nascent EPBs are produced by magnetic activity of category E; in case b the effect seen in the equatorial ionosphere could be associated with

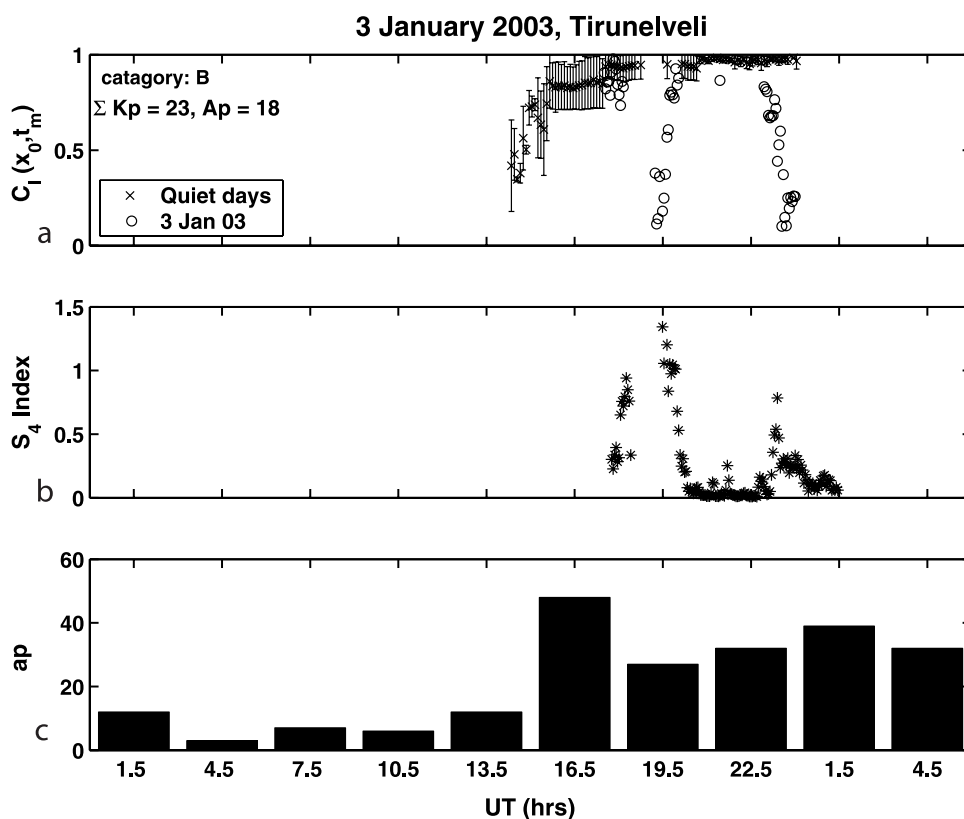


Figure 3. Plot of (a) monthly quiet time average of $C_I(x_0, t_m)$ with standard deviation for January 2003 superposed with disturbed time $C_I(x_0, t_m)$, (b) S_4 index, and (c) ap indices on 3 January 2003 (Category B) as a function of UT.

magnetic activity of category C or D; i.e., these are the two categories where the observed nascent EPBs could be produced only through disturbance dynamo effects. The categories A and B are associated with the ionospheric effects seen in case a, where it is not possible to separate the effect of prompt penetration electric field from that of a disturbance dynamo electric field. Since the conductivity distribution and neutral winds determine the nature of the disturbance electric field in equatorial ionosphere, seasonal variation is expected in the generation of EPBs due to the effects of magnetic activity listed above under cases a and b. Hence for each of these cases, the magnetically disturbed days with scintillation are divided into different seasons. As an example, Figure 5 shows the distribution of $C_I(x_0, t_m)$ with local time on quiet and disturbed days for the equinoctial months of September and October. Figures 5a, 5b, and 5c show quiet days, disturbed days of categories A to D, and isolated prompt penetration cases, respectively. The colors indicate different levels of $C_I(x_0, t_m)$. The quiet time data set for equinoctial period (September and October) consists of 85 days with observed scintillations and the disturbed time data set is composed of 49 days with scintillation occurrence. From Figure 5 it is clear that low values of $C_I(x_0, t_m) < (0.7)$ prevail for less than 2 hours during the postsunset period, rarely extending beyond 2200 LT, on magnetically quiet days, whereas prolonged periods of low $C_I(x_0, t_m)$ are observed on magnetically disturbed days even after 2200 LT.

[19] As discussed earlier, low values of $C_I(x_0, t_m)$ are associated with freshly generated irregularities. Hence percentage occurrence pattern of $C_I(x_0, t_m) \leq 0.5$ for equinoctial and solstice months for magnetically quiet and disturbed periods may be used as a proxy for studying the generation of fresh irregularities due to growth of R-T instability at different local times during different seasons. The percentage occurrence pattern of $C_I(x_0, t_m) \leq 0.5$ as a function of local time for magnetically quiet and for disturbed days divided into cases a, b, and c are shown in Figure 6, showing results for autumnal (September and October) (left) and vernal (March and April) (right) equinoxes, respectively. Similar plot of percentage distribution of $C_I(x_0, t_m) \leq 0.5$ as a function of LT is shown for solstice months November, December, January, and February (right) and May, June, July, and August (left) in Figure 7. It should be noted that even though the number of quiet days is always more than the number of disturbed days, with each scintillation interval of 3 min duration with $C_I(x_0, t_m) \leq 0.5$ constituting one data point, the number of data points is always more during magnetically active periods than during magnetically quiet periods, for all seasons. This is because during magnetically quiet times, intervals with $C_I(x_0, t_m) \leq 0.5$ occur mostly before 2200 LT, indicating that fresh generation of ESF irregularities does not take place after 2200 LT in all seasons. On the other hand, disturbed time statistical pattern of occurrence of intervals with $C_I(x_0, t_m) \leq 0.5$ shows fresh generation of ESF irregularities after 2200 LT as well. In

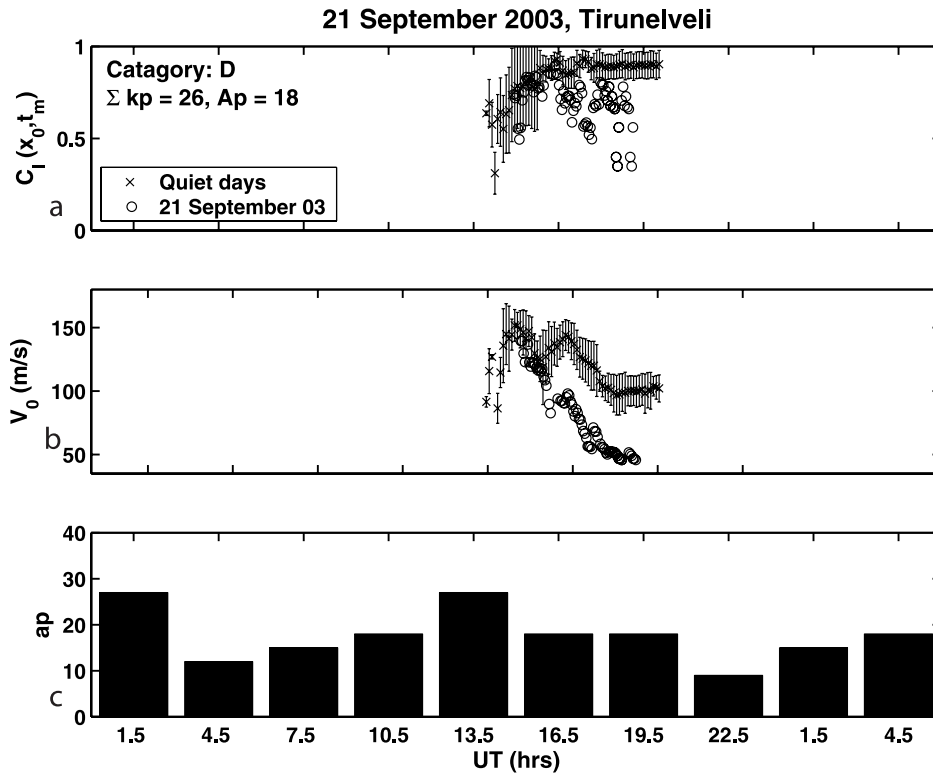


Figure 4. Plot of monthly quiet time average of (a) $C_I(x_0, t_m)$, (b) drift speed of ground scintillation pattern V_0 , with standard deviation for September 2003, superposed with disturbed time $C_I(x_0, t_m)$ and V_0 , respectively, on 21 September 2003 versus UT, and (c) distribution of ap versus UT for 21 September 2003 (category D).

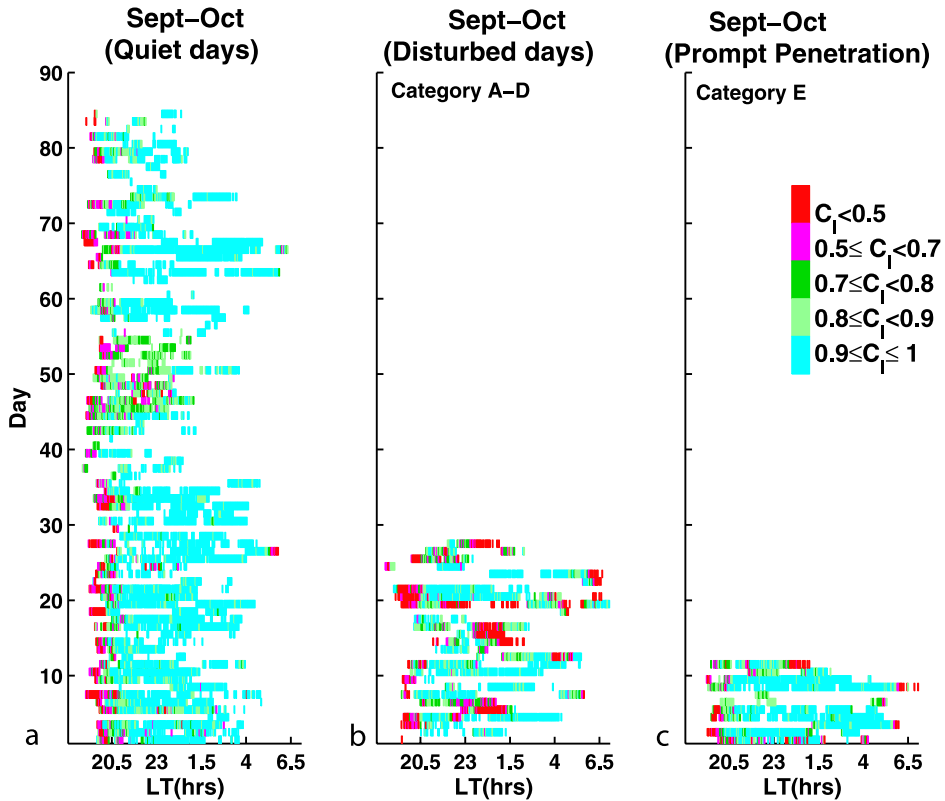


Figure 5. Distribution of $C_I(x_0, t_m)$ with local time for (a) quiet days, (b) disturbed days from category A, B, C, and D, and (c) isolated prompt penetration cases (category E) for equinoctial months September and October. Color scale indicate the different level of $C_I(x_0, t_m)$.

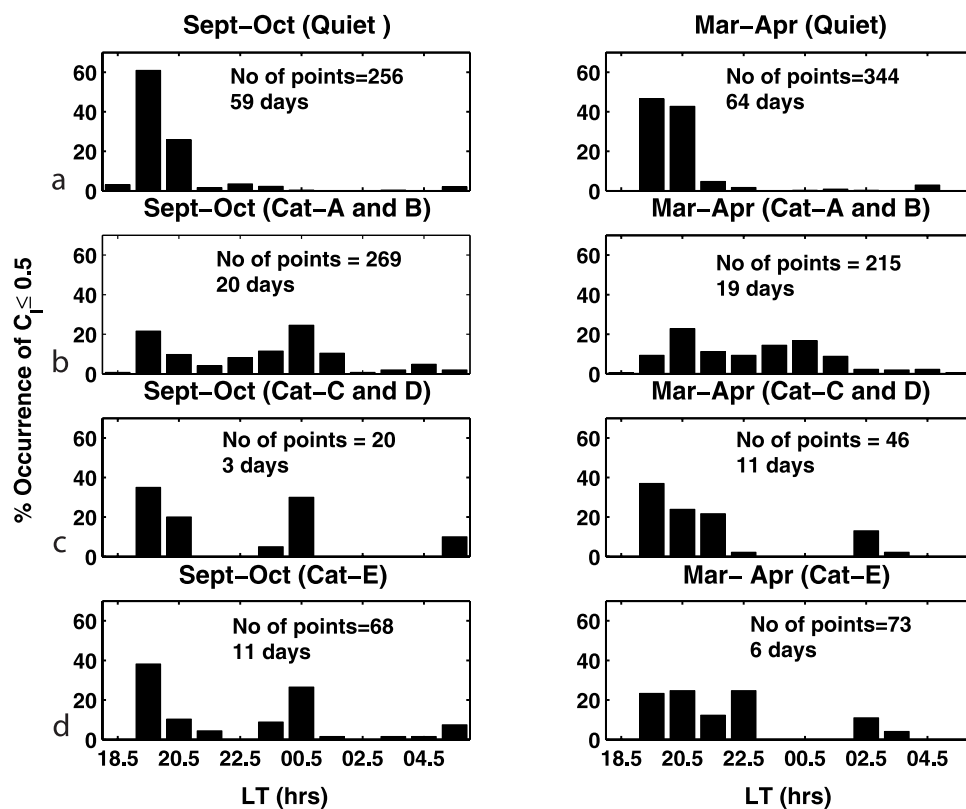


Figure 6. Percent occurrence pattern of $C_I(x_0, t_m) \leq 0.5$ with local time for (a) quiet days, (b) disturbed days, which shows effect of disturbance dynamo and prompt penetration both (category A and B), (c) disturbed days, which shows effect of disturbance dynamo (category C and D), and (d) disturbed days associated with only prompt penetration of electric field (category E), for September and October and March and April equinox.

September and October equinoctial period, percentage occurrence of $C_I(x_0, t_m) \leq 0.5$ maximizes around midnight for all three cases a, b, and c, indicating that the probability of fresh generation of ESF irregularities is maximum at midnight in this season. Surprisingly, for March and April, fresh generation of EPBs, which may be attributed to either prompt penetration electric field or disturbance dynamo electric field acting separately, tends to peak at a later time around 0230 LT as compared to a midnight peak during autumnal equinox. Clear disturbance dynamo cases are too few for summer solstice months, but winter solstice also show a similar pattern of occurrence as the vernal equinox. However for prompt penetration cases, the summer solstice shows peak generation of fresh EPBs around midnight. In all seasons, case a, where it is difficult to separate the prompt penetration effects from disturbance dynamo effects, the pattern of fresh generation of EPBs differs from that seen in either case b or c. This may be a consequence of promptly penetrating electric fields causing alteration in the F region electron density, Pedersen conductivity distribution of midlatitude and low-latitude ionosphere, and ion drag on the neutrals in such a way as to also cause changes in the development of disturbance dynamo [Maruyama *et al.*, 2005]. A study by Sobral *et al.* [1997] suggests that occasionally effect of disturbance dynamo and prompt penetration electric fields can partially or completely cancel

each other, and as a result postsunset prereversal enhancement of electric field is unaffected even during magnetically active periods in such situations.

[20] In Figures 6 and 7, for days with categories A, B, and C of magnetic activity, the possibility of the previous day being magnetically active has not been excluded. Hence for these days, some of the observed effects on the equatorial ionosphere may arise from disturbance dynamo set up by magnetic disturbances of the previous day. In order to examine the extent of contribution of magnetic activity of the previous day to the generation of fresh EPB on days with category A or B magnetic activity (there are very few days in category C and hence these days have been excluded), the occurrence pattern of 3 min intervals with $C_I(x_0, t_m) \leq 0.5$ at different local time on such days (A + B) is shown in Figure 8 for both equinoxes and solstice, under three different conditions of magnetic activity on the previous day: (1) no magnetic activity; (2) category A magnetic activity; and (3) category B magnetic activity. It is clear that for solstice, increased probability of fresh generation of EPBs around midnight arises from disturbances dynamo effects of magnetic activity of the previous day. This feature may be related to storm-driven compositional changes that occur in middle and low latitudes during solstices [Fuller-Rowell *et al.*, 1996]. For equinoxes, the increased generation of EPBs around midnight is mostly the result of

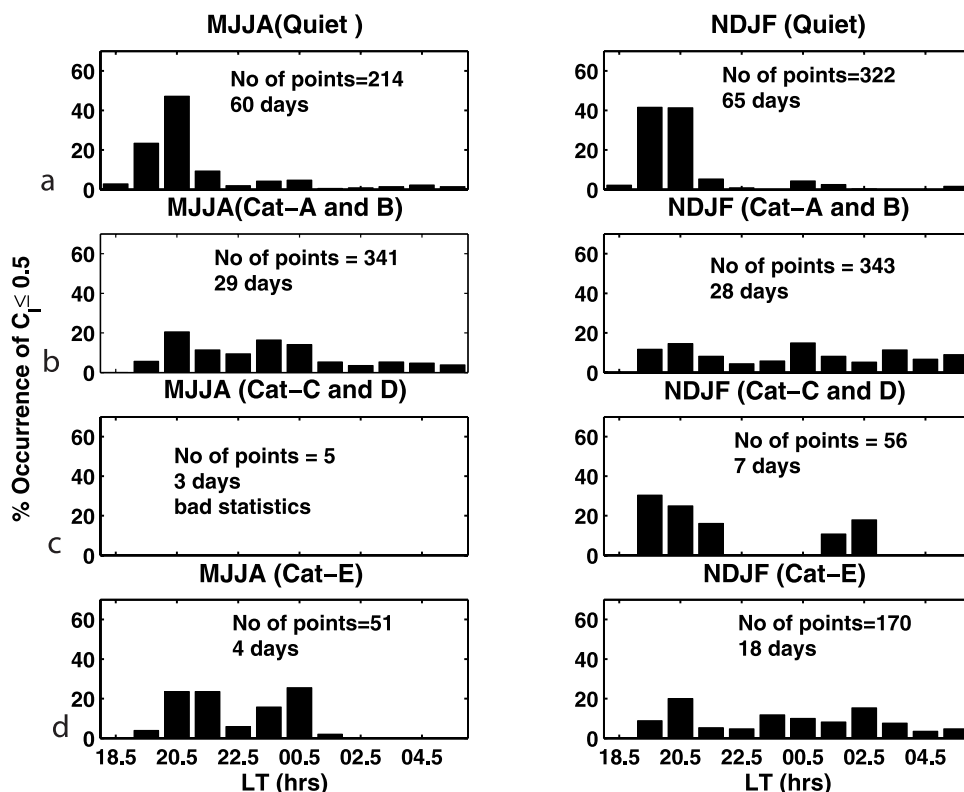


Figure 7. Percent occurrence pattern of $C_I(x_0, t_m) \leq 0.5$ with local time for (a) quiet days, (b) disturbed days, which shows effect of disturbance dynamo and prompt penetration both (category A and B), (c) disturbed days, which shows effect of disturbance dynamo (category C and D), and (d) disturbed days associated with only prompt penetration of electric field (category E), for May through August and November through February solstice.

combination of prompt penetration and disturbance dynamo effects associated with magnetic activity that takes place on the day under consideration.

[21] As has been noted earlier, height of the equatorial F layer during postsunset hours plays an important role in fresh generation of ESF irregularities. Turning of westward electric field to eastward raises the F layer to higher heights, where conditions are favorable for the growth of the R-T plasma instability and this leads to fresh generation of irregularities. Though the magnetically disturbed days considered in a given season have different past histories, which would get reflected in statistical occurrence patterns of $C_I(x_0, t_m) \leq 0.5$, the increased tendency towards fresh generation of irregularities around midnight is observed in almost all the seasons. This indicates that the probability of electric field turning from westward to eastward is highest around midnight during magnetically disturbed periods. Simulation results of *Richmond et al.* [2003] suggest that disturbed winds drive an equatorward dynamo current that allows the building up of positive charges in the equatorial ionosphere around midnight, which leads to reversal of perturbed westward electric field to eastward around this time. A recent study by *Huang et al.* [2005] also suggests that local time for reversal of disturbance dynamo perturbation electric field from westward to eastward is close to local midnight with some longitudinal variation. Significant suppression of the fresh generation of scintillation producing irregularities immediately following postsunset period is

clearly observed during vernal equinox (March and April) and to a lesser extent during solstice months, but it is not observed for autumnal equinox (September and October).

6. Summary

[22] In this paper a large database of spaced receiver scintillation observations has been used to study the effect of magnetic activity on the generation of irregularities in the nighttime equatorial ionosphere, which are capable of producing scintillations on transionospheric VHF signals. The first step in this study was to resolve the important issue of identification of freshly generated EPBs using spaced receiver scintillation observations. The local time distribution of the maximum cross correlation $C_I(x_0, t_m)$ of scintillations recorded by two spaced receivers is different for magnetically disturbed and quiet periods. Low values of $C_I(x_0, t_m)$ observed after 2200 LT during magnetically disturbed days are not seen on magnetically quiet days, and as discussed in the introduction this parameter has been shown to be a good indicator of freshly generated EPBs in which the perturbation electric field associated with the R-T instability give rise to random movement of the irregularities with respect to the background plasma [*Bhattacharyya et al.*, 1989, 2001, 2002]. This is the first time that this technique has been used in a statistical study of the effect of magnetic activity on the generation of EPBs. The strength and extent of the effect of magnetic activity on the equato-

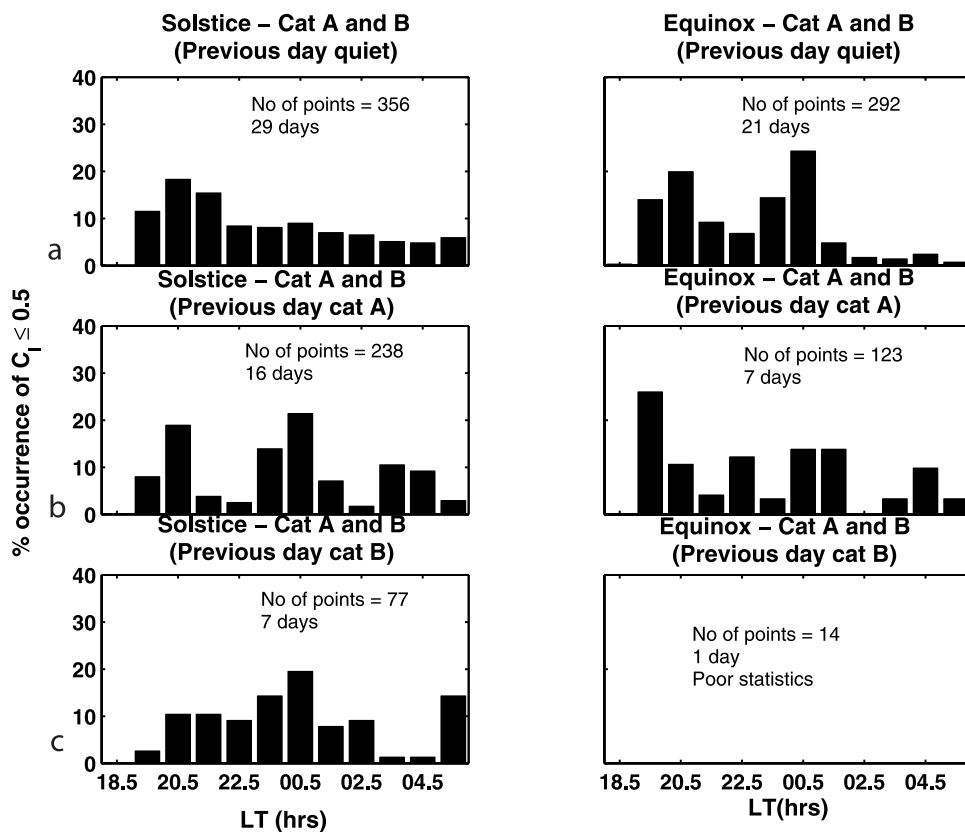


Figure 8. Percent occurrence pattern of $C_I(x_0, t_m) \leq 0.5$ as a function of LT for magnetically disturbed days, which show a combined effect of disturbance dynamo and prompt penetration electric field (category A and B), when previous day is associated with (a) no magnetic activity, (b) magnetic activity of category A, and (c) magnetic activity of category B, for solstice (November through February, May through August) and equinoctial months (March through April, September through October).

rial ionosphere depends on the morphology of magnetic disturbances and their time evolution. Magnetic activity may suppress or initiate the growth of R-T plasma instability on the bottomside of the equatorial postsunset F region depending on the modulation of the equatorial ionospheric zonal electric field by the magnetic activity. Although magnetically disturbed days show a wide range of characteristics, and their effects in the postsunset equatorial ionosphere are also expected to show seasonal variation, all the seasons show an increase in occurrence of $C_I(x_0, t_m) \leq 0.5$ around midnight, with a clearly enhanced peak during the equinoctial months of September and October.

[23] As far as disturbance dynamo electric fields are concerned, *Scherliess and Fejer* [1999] have shown using long-term radar observations at Jicamarca that the efficiency of the disturbance dynamo in producing eastward electric fields in the equatorial region is highest around midnight for effects seen with a delay of 5–10 hours or on the day after high-latitude current enhancement with a delay of 22–28 hours, while the efficiency is highest around 0230 LT for effects seen with delays of less than 5 hours. Model calculations by *Richmond et al.* [2003] and *Huang et al.* [2005] show that the westward to eastward turning of ionospheric electric field due to a disturbance dynamo, is likely to occur around local midnight. Results presented here support the theoretical model calculations, since an

equatorial eastward electric field will raise the equatorial F layer to a higher height, where the growth rate of R-T instability is higher and this leads to generation of EPBs. Considering the days when the effect of magnetic activity on the equatorial ionospheric zonal electric field may be attributed to disturbance dynamo alone, there is a significant difference in the time of maximum generation of fresh EPB between autumnal and vernal equinoxes. In all the seasons, the days for which there is a possibility of overlap of prompt penetration of high latitude electric field to the equatorial ionosphere with a disturbance dynamo, the pattern of generation of fresh irregularities is significantly different from that found when only disturbance dynamo effects are seen. This supports the results of *Maruyama et al.* [2005] obtained by modeling a magnetic storm, that a promptly penetrated electric field has a considerable impact on the disturbance dynamo at nighttime. For magnetically disturbed days in categories A and B with magnetic activity starting at different times, days with and without magnetic activity on previous day show significantly different occurrence patterns of freshly generated irregularities. These results show that during solstice, disturbance dynamo effects related to storm driven compositional changes that occur in middle and low latitudes, may result in eastward electric fields around midnight, creating right conditions for generation of EPBs. On the other hand for equinoxes, the

increased generation of EPBs around midnight may be the result of a combination of prompt penetration and short term disturbance dynamo electric fields associated with magnetic activity that takes place on the day under consideration. It should be stated here that the statistics of fresh generation of EPBs is shown separately for different seasons so that possible seasonal effects do not mask the greater probability of such generation at particular local times. However, at this stage it is not possible to provide an explanation for the seasonal differences, which would require detailed modeling using background conductivity distribution appropriate for a particular season.

[24] **Acknowledgments.** Amitava Bhattacharjee thanks the reviewers for their assistance in evaluating this paper.

References

- Akasofu, S. I. (1981), Energy coupling between the solar wind and the magnetosphere, *Space Sci. Rev.*, *28*, 121–190.
- Bartels, J. (1957), The technique of scaling indices K and Q of geomagnetic activity, *Ann. Int. Geophys. Year*, *4*, 215–226.
- Basu, S., et al. (1996), Scintillations, plasma drifts, and neutral winds in the equatorial ionosphere after sunset, *J. Geophys. Res.*, *101*(A12), 2,6795–26,810.
- Basu, S., Su. Basu, K. M. Groves, E. MacKenzie, M. J. Keskinen, and F. J. Rich (2005), Near-simultaneous plasma structuring in the midlatitude and equatorial ionosphere during magnetic superstorm, *Geophys. Res. Lett.*, *32*, L12S05, doi:10.1029/2004GL021678.
- Basu, Su., et al. (2005), Two components of ionospheric plasma structuring at midlatitudes observed during the large magnetic storm of October 30, 2003, *Geophys. Res. Lett.*, *32*, L12S06, doi:10.1029/2004GL021669.
- Bhattacharyya, A., S. J. Franke, and K. C. Yeh (1989), Characteristic velocity of equatorial *F* region irregularities determined from spaced receiver scintillation data, *J. Geophys. Res.*, *94*(A9), 11,959–11,969.
- Bhattacharyya, A., S. Basu, K. M. Groves, C. E. Valladares, and R. Sheehan (2001), Dynamics of equatorial *F* region irregularities from spaced receiver scintillation observations, *Geophys. Res. Lett.*, *28*(1), 119–122.
- Bhattacharyya, A., S. Basu, K. M. Groves, C. E. Valladares, and R. Sheehan (2002), Effect of magnetic activity on the dynamics of equatorial *F* region irregularities, *J. Geophys. Res.*, *107*(A12), 1489, doi:10.1029/2002JA009644.
- Blanc, M., and A. D. Richmond (1980), The ionospheric disturbance dynamo, *J. Geophys. Res.*, *85*, 1669–1686.
- Brigg, B. H. (1984), The analysis of spaced sensor records by correlation techniques, in *Middle Atmosphere Program, Handbook for MAP*, vol. 13, edited by R. A. Vincent, pp. 166–186, Int. Council of Sci. Unions, Paris.
- Dymond, K. F., S. A. Budzien, A. C. Nicholas, S. E. Thonnard, R. P. McCoy, R. J. Thomas, J. D. Huba, and G. Joyce (2004), Ionospheric response to the solar flare of 14 July 2000, *Radio Sci.*, *39*, RS1S25, doi:10.1029/2002RS002842.
- Engavale, B., K. Jeeva, K. U. Nair, and A. Bhattacharyya (2005), Solar flux dependence of coherence scales in the scintillation pattern produced by ESF irregularities, *Ann. Geophys.*, *23*, 3261–3266.
- Fejer, B. G., and L. Scherliess (1995), Time dependent response of equatorial ionospheric electric fields to magnetospheric disturbances, *Geophys. Res. Lett.*, *22*(7), 851–854.
- Fejer, B. G., R. W. Spiro, R. A. Wolf, and J. C. Foster (1990), Latitudinal variation of perturbation electric fields during magnetically disturbed periods: 1986 SUNDIAL observations and model results, *Ann. Geophys.*, *8*, 441–454.
- Fejer, B. G., E. R. de Paula, S. A. Gonzalez, and R. F. Woodman (1991), Average vertical and zonal *F* region plasma drifts over Jicamarca, *J. Geophys. Res.*, *96*(A8), 13,901–13,906.
- Fejer, B. G., L. Scherliess, and E. R. de Paula (1999), Effects of the vertical plasma drift velocity on the generation and evolution of equatorial spread *F*, *J. Geophys. Res.*, *104*, 19,859–19,869.
- Fuller-Rowell, T. J., M. V. Codrescu, H. Risbeth, R. J. Moffett, and S. Quegan (1996), On the seasonal response of the thermosphere and ionosphere to geomagnetic storms, *J. Geophys. Res.*, *101*(A2), 2343–2354.
- Fuller-Rowell, T. J., G. H. Millward, A. D. Richmond, and M. V. Codrescu (2002), Storm-time changes in the upper atmosphere at low latitudes, *J. Atmos. Sol. Terr. Phys.*, *64*, 1383–1391.
- Huang, C. M., A. D. Richmond, and M. Q. Chen (2005), Theoretical effects of geomagnetic activity on low-latitude ionospheric electric fields, *J. Geophys. Res.*, *110*, A05312, doi:10.1029/2004JA010994.
- Jayachandran, B., N. Balan, P. B. Rao, J. H. Sastri, and G. J. Bailey (1993), HF Doppler and ionosonde observations on the onset conditions of equatorial spread *F*, *J. Geophys. Res.*, *98*, 13,741–13,760.
- Lopez, R. E., M. Wiltberger, S. Hernandez, and J. G. Lyon (2004), Solar wind density control of energy transfer to magnetosphere, *Geophys. Res. Lett.*, *31*, L08804, doi:10.1029/2003GL018780.
- Maruyama, N., A. D. Richmond, T. J. Fuller-Rowell, M. V. Codrescu, S. Sazykin, F. R. Toffoletto, R. W. Spiro, and G. H. Millward (2005), Interaction between direct penetration and disturbance dynamo electric fields in the storm-time equatorial ionosphere, *Geophys. Res. Lett.*, *32*, L17105, doi:10.1029/2005GL023763.
- Menvielle, M., and A. Berthelier (1991), The K-derived planetary indices: description and availability, *Rev. Geophys.*, *29*(3), 415–432.
- Retterer, J. M. (1999), Theoretical model for fast equatorial bubbles, paper presented at Ionospheric Effects Symposium, Off. of Naval Res., Alexandria, Va.
- Richmond, A. D., C. Peymirat, and R. G. Roble (2003), Long-lasting disturbances in the equatorial ionospheric electric field simulated with a coupled magnetosphere-ionosphere-thermosphere model, *J. Geophys. Res.*, *108*(A3), 1118, doi:10.1029/2002JA009758.
- Scherliess, L., and B. G. Fejer (1999), Radar and satellite global equatorial *F* region vertical drift model, *J. Geophys. Res.*, *105*, 6829–6842.
- Sobral, J. H. A., M. A. Abdu, W. D. Gonzalez, B. T. Tsurutani, I. S. Batista, and A. L. Clua de Gonzalez (1997), Effects of intense storms and substorms on the equatorial ionosphere/thermosphere system in the American sector from ground-based and satellite data, *J. Geophys. Res.*, *102*(A7), 14,305–14,314.
- Spiro, R. W., R. A. Wolf, and B. G. Fejer (1988), Penetration of high-latitude electric field effects to low latitude during SUNDIAL 1984, *Ann. Geophys.*, *6*, 39–50.
- Valladares, C. E., R. Sheehan, S. Basu, H. Kuenzler, and J. Espinoza (1996), The multi-instrumented studies of equatorial thermosphere aeronomy scintillation system: Climatology of zonal drifts, *J. Geophys. Res.*, *101*(A12), 26,839–26,850.

A. Bhattacharyya, K. Jeeva, B. Kakad, and K. U. Nair, Indian Institute of Geomagnetism, Navi Mumbai, New Panvel, India, 410218. (ebharati@iigs.iigs.res.in)